

MLS OBSERVATIONS OF STRATOSPHERIC WAVES IN
TEMPERATURE AND O_3 DURING THE 1992 SOUTHERN WINTER

E.F. Fishbein, L. S. Elson, L. Froidevaux, G.L. Manney, W.G. Read,
J. W. Waters and R. W. Zurek

Jet Propulsion Laboratory, California Institute of Technology, Pasadena CA

Abstract. The Microwave Limb Sounder observed waves in stratospheric temperature and O_3 during the 1992 southern winter. Wave 1 intensifies three times from mid August through mid September, resulting in three minor sudden warmings and increased zonal mean O_3 , when a 9 day eastward traveling wave becomes in phase with the stationary wave 1. When the waves are in phase, an intensified baroclinic zone arises from the wave's westward phase tilt. Ozone wave amplitudes near 5 - 10 hPa intensify during the warmings and are larger than expected from photochemistry alone, implying transport by planetary waves; this is supported by positive phase correlation between the waves in O_3 and temperature.

Introduction

An analysis of the LIMS data set [Leovy et al., 1985] showed that the ozone distribution is strongly affected by planetary waves, leading to poleward transport of ozone during sudden warmings. Another example, the 1988 sudden warmings of the southern polar stratosphere [Kanzawa and Kawaguchi, 1990; Schoeberl et al., 1989], led to an anomalously weak ozone hole that year. The 1992 southern winter experienced several minor warmings at a time when increases in O_3 were associated with transport into the vortex [Manney et al. submitted to this issue]. It is expected that O_3 transport is related to the planetary waves associated with these warmings.

This letter describes observed wave activity associated with the 1992 southern winter warmings and its role in transporting ozone into the vortex. The data consist of

Microwave Limb Sounder (MLS) measurements of temperature (T) and O₃ concentration during the period from 14 August through 20 September 1992, retrieved as described by Waters et al. [1993]. The useful vertical coverage with current MLS algorithms (UARS version 0003 products) is 20 to 0.2 hPa for T, and 100 to 0.2 hPa for O₃. MLS temperatures are supplemented below 20 hPa by National Meteorological Center (NMC) 1200Z daily analyses sampled along the MLS measurement track. MLS data validation to date shows zonal mean agreement with NMC temperatures to 1-2 K between 10 and 1 hPa, and with ozonesondes and SAGE O₃ measurements to better than 10% between 50 and 1 hPa. Fourier coefficients in time and longitude, are evaluated using the Salby method [1982], as described by Elson et al. [1993]. The measurement geometry allows resolution of zonal wavenumbers ≤ 7 and frequencies (periods) from 0.028/day (36.1 day) to 1.04/day (0.96 day).

Observations and Discussion

Figure 1 shows T and O₃ zonal means at 5, 10 and 50 hPa. Three warmings, ~ 9 days apart are seen at 5 hPa and 10 hPa, and to a lesser extent at 50 hPa. The second warming has the largest temperature increase (18 K at 75S and 5 hPa) developing over 3 days starting on 2 September (1992-246). Warming begins in the mid-stratosphere above 10 hPa and propagates into the lower stratosphere ~ 1 day later. The southern mid-latitude stratosphere to 20° S and the polar mesosphere south of 60° S experience cooling during the warmings. During the warmings, zonal-mean O₃ mixing ratio south of 60° S increases at 5 and 10 hPa. The O₃ mixing ratio increases are largest during the second warming, showing a 1.5 ppmv increase at 75° S and 5 hPa.

Figure 2 shows the power spectra of the time series of T and O₃ zonal waves 1 and 2 at 75° S over a vertical range from 50 to 0.2 hPa. The power spectra are typical for the southern winter, containing primarily stationary and eastward-propagating traveling waves [Meechoso and Hartman, 1982; Manney et al. 1991]. Zonal wave 1 has most of its power in a stationary wave, and 9 and 4.5 day eastward traveling waves. Wave 2 has no stationary component but has traveling components with the same periods as wave 1. Wave 2 is unusual this year in that its amplitude is considerably smaller than wave 1 [Manney et

al., 1991].

At 20 and 50 hPa, the presence of ClO during this period [Waters et al., submitted to this issue] indicates chemical loss due to processes triggered by heterogeneous chemistry. The dissimilarity of O₃ and 'T' time series spectra at these pressures is consistent with the O₃ field transitioning from a transport-dominated regime to one dominated by O₃ loss.

in the Matsuno [1971] model of sudden warmings, the mean field is perturbed by waves having growing amplitudes. Figure 3 shows the amplitude of wave 1 at 75° S and 5 hPa during the period of observation. During each of the warmings, wave 1 intensifies in both T and O₃ but the intensification of wave 1 in O₃ lags behind the wave in 'T'. The amplitudes of the 9 and 4.5 day traveling waves, obtained by Gaussian bandpass filtering the spectra (0.04/day half width at half-maximum) are also shown. The 9 day wave, seen in both T and O₃, intensifies throughout the beginning of the observation period, reaching maximum amplitude during the second warming. The 4.5 day wave shows similar behavior, although the intensifications are more localized near the warming. Although the 4.5 day wave intensifies before the 9 day wave, there is no indication that the traveling waves in O₃ lag behind 'T'.

Figure 3 also shows the amplitude of the sum of each traveling wave and the stationary wave (i.e. the waves are added taking into account their phases). Maxima occur when the traveling waves become in phase with the stationary wave, once every 9 days. These coincide with the warmings, showing that a major source of wave intensification arises from beating between the waves. The wave amplitudes in the O₃ field shows similar behavior, except that maximum amplitude occurs after the temperature waves.

The phase of the waves during the second warming (4 September at 0930Z) is shown in figure 4. The waves are approximately in phase as indicated by figure 3, but, because the phase height relations are slightly different, the waves are in phase 1 day later at 50 hPa relative to 2 hPa; the same time delay is seen in the zonal mean warming. The amplitude of the O₃ wave 1 increases after 'T' because the phases of the O₃ and 'T' waves are slightly different, resulting in the waves in O₃ coming in phase later.

'T' traveling and stationary waves have westward phase tilt

resulting in a baroclinic zone (regions of strong vertical and horizontal 'J' gradients tilting westward with height). As the traveling wave moves into phase with the stationary wave, the baroclinic zone intensifies. Figure 5 shows temperature cross-sections during the second warming and 4.5 days later when the waves are out of phase. The baroclinic zone is strongest during the warming, but is almost absent 4.5 days later. Fairlie et al.'s [1990] simulation of a northern hemisphere major stratospheric warming showed that formation of baroclinic zones resulted in an ageostrophic flow and deceleration of the polar vortex. Baroclinic zones can generate small scale waves and therefore could provide an energy source for intensifying the 9 and 4.5 day traveling waves. Strong downward motions are often produced by baroclinic zones [Fairlie et al., 1990], so warming from downward motions may be present.

The question arises as to whether the O_3 waves result from photochemistry or transport. The photochemistry of O_3 is strongly temperature dependent and produces anti-correlations between T and O_3 concentration [Froidevaux et al., 1989]. The correlation between O_3 and '1' waves is the cosine of the phase difference between the waves which can be obtained from figure 4. Between 2 and 10 hPa, the stationary and traveling waves are positively correlated (>0.5 at 5 and 10 hPa), inconsistent with photochemistry. The amplitude of the photochemical O_3 response to a sinusoidal temperature perturbation is also much smaller than is observed. Following the linearized treatment of Froidevaux et al. [1989], the O_3 perturbation from a 6 K temperature perturbation with a 9 day period are approximately 90 and 5 ppbv at 5 and 10 hPa (using 10 day and 100 day photochemical timescales). These amplitudes are approximately 10 and 100 times smaller than observed, suggesting that dynamical terms not considered in the above are the source of the observed large O_3 variation. As with temperature, although horizontal motions are one source of O_3 transport, [Manney et al., submitted this issue], vertical transport may be important.

Conclusions

Stratospheric wave activity in the south during August and September 1992 was dominated by zonal wave 1 consisting of stationary and 9 day eastward-traveling components. Consistent with the Matsuno mode 1 of stratospheric,

warming, wave 1 intensified during the warmings. Wave 1 was intensified primarily by wave interactions between the traveling and stationary components, but the individual traveling waves also intensified during the study period. This may have been caused by a baroclinic zone which was created by the waves and intensified whenever the waves were in phase. Wave 2 does not play a major role in the warmings.

Many similarities were seen between O_3 and T at 5 and 10 hPa. The zonal mean heating and O_3 concentration were positively correlated. Both showed the same wave components, and in each, the waves intensified during the warmings. The correlation between T and O_3 waves and the ratio of spectra indicated that the waves in O_3 were not a result of normal photochemistry, but indicated O_3 transport. The effects of the baroclinic zone on transport have not been ascertained, but winds derived from it may have transported O_3 both horizontally and vertically.

Sudden warmings disrupted the vortex in late winter 1988 and 1992, but unlike 1988, the 1992 O_3 hole became stronger than the previous year [CAC, 1992]. In 1988 the rate of O_3 decline was halted soon after the warmings [Schoeberl et al., 1988; Kanzawa and Kawaguchi, 1990], but as seen in figure 1, 46 hPa zonal mean O_3 continued to decrease through the remainder of the study period. In summary, although wave activity associated with sudden warmings can increase O_3 in the vortex, the presence of warmings does not imply a weakened hole. Further study should provide additional information on the couplings between wave activity, sudden warmings, and the depth and duration of the ozone hole.

Acknowledgments. We thank our many colleagues and the entire MISTeam for their support and contributions. This work was performed by the Jet Propulsion Laboratory, California Institute of Technology, under contract with the National Aeronautics and Space Administration.

References

- Climate Analysis Center (CAC), *Southern Hemisphere Winter Summary*, National Oceanic and Atmospheric Administration, 1992.
- Elson, L. S., J. W. Waters, and I. Froidevaux, The use of Fourier transforms for synoptic mapping: Early results from the Upper Atmosphere Research Satellite Mi-

- crowave Limb Sounder, *J. Geophys. Res.*, submit, ted 1993.
- Fairlie, T., M. Fisher, and A. O'Neill, The development of narrow baroclinic zones and other small-scale structure in the stratosphere during simulated major warmings, *Q. J. Roy. Meteor. Soc.*, 116, 287-315, 1990.
- Froidevaux, L., M. Allen, S. Berman, and A. Daughton, The mean ozone profile and its temperature sensitivity in the upper stratosphere and lower mesosphere: An analysis of LIMS observations, *J. Geophys. Res.*, 94, 6389-6417, 1989.
- Kanzawa, H. and S. Kawaguchi, Large stratospheric sudden warming in antarctic late winter and shallow ozone hole in 1988, *Geophys. Res. Lett.*, 17, 77-80, 1990.
- Leovy, C., C.-R. Sun, M. Hitchman, E. Remsberg, J. R. III, L. Gordley, J. Gille, and L. Lyjak, Transport of O_3 in the middle stratosphere: Evidence for planetary wave breaking, *J. Atmos. Sci.*, 42, 230-244, 1985.
- Manney, G., J. Farrara, and C. Mechoso, The behavior of wave 2 in the southern hemisphere stratosphere during late winter and early spring, *J. Atmos. Sci.*, 48, 976-998, 1991.
- Manney, G. L., L. Froidevaux, J. W. Waters, L. S. Elson, E. F. Fishbein, R. W. Zurek, R. S. Harwood, and W. A. Lahoz, The evolution of ozone observed by UARS MLS in the 1992 late winter southern polar vortex, *Geophys. Res. Lett.*, submitted 1993.
- Matsuno, T., A dynamical model of the stratospheric sudden warming, *J. Atmos. Sci.*, 28, 1479-1494, 1971.
- Mechoso, C. and D. Hartmann, An observational study of traveling planetary waves in the southern hemisphere, *J. Atmos. Sci.*, 39, 1921-1935, 1982.
- Salby, M. L., Sampling theory for synoptic satellite observations. Part I: Space-time spectra, resolution and aliasing, *J. Atmos. Sci.*, 39, 2577-2600, 1982.
- Schoeberl, M. J., R. S. Stolarski, and A. J. Krueger, The 1988 Antarctic ozone depletion: Comparison with previous year depletions, *Geophys. Res. Lett.*, 16, 377-380, 1989.
- Waters, J. W., L. Froidevaux, W. G. Read, G. L. Manney, L. S. Elson, D. A. Flower, R. F. Jarnot, and R. S. Harwood, Stratospheric chlorine monoxide and ozone: First results from UARS MLS, *Nature*, submitted, 1993.
- Waters, J. W., C. J. Manney, W. G. Read, L. Froidevaux, and L. S. Elson, Lower stratospheric ClO and O_3 in the

1992 southern hemisphere winter, *Geophys. Res. Lett.*,
submitted 1993.

Fig. 1. Zonal means of temperature at 5 hPa (a), 10 hPa (b) and 50 hPa (c) and of O₃ at the same pressures (d,e,f).

Fig. 2. Wave amplitude spectra versus frequency and height at 75° S for T (a,b) and O₃ (c,d) for zonal wavenumbers 1 (a,c) and 2 (b,d).

Fig. 3. The evolution of T (a) and O₃(b) wave amplitude for zonal wavenumber 1 at 75° S and 5 hPa. Shown are amplitudes of all spectral components (solid), eastward-propagating 9 day wave (dashed), eastward-propagating 4.5 day wave (dotted), stationary plus 9 day component (3 dot-dash) and stationary plus 4.5 day wave component (dot-dash).

Fig. 4. The longitude of the wave crest versus height of the stationary wave (diamonds) and the 9 day eastward-propagating wave (triangles) for T (solid line) and O₃ (dashed line) on 4 September at 0930Z.

Fig. 5. The temperature cross-section at 75° S on (a) 4 September 1992 at 1000Z, and (b) 9 September 1992 at 0000Z.

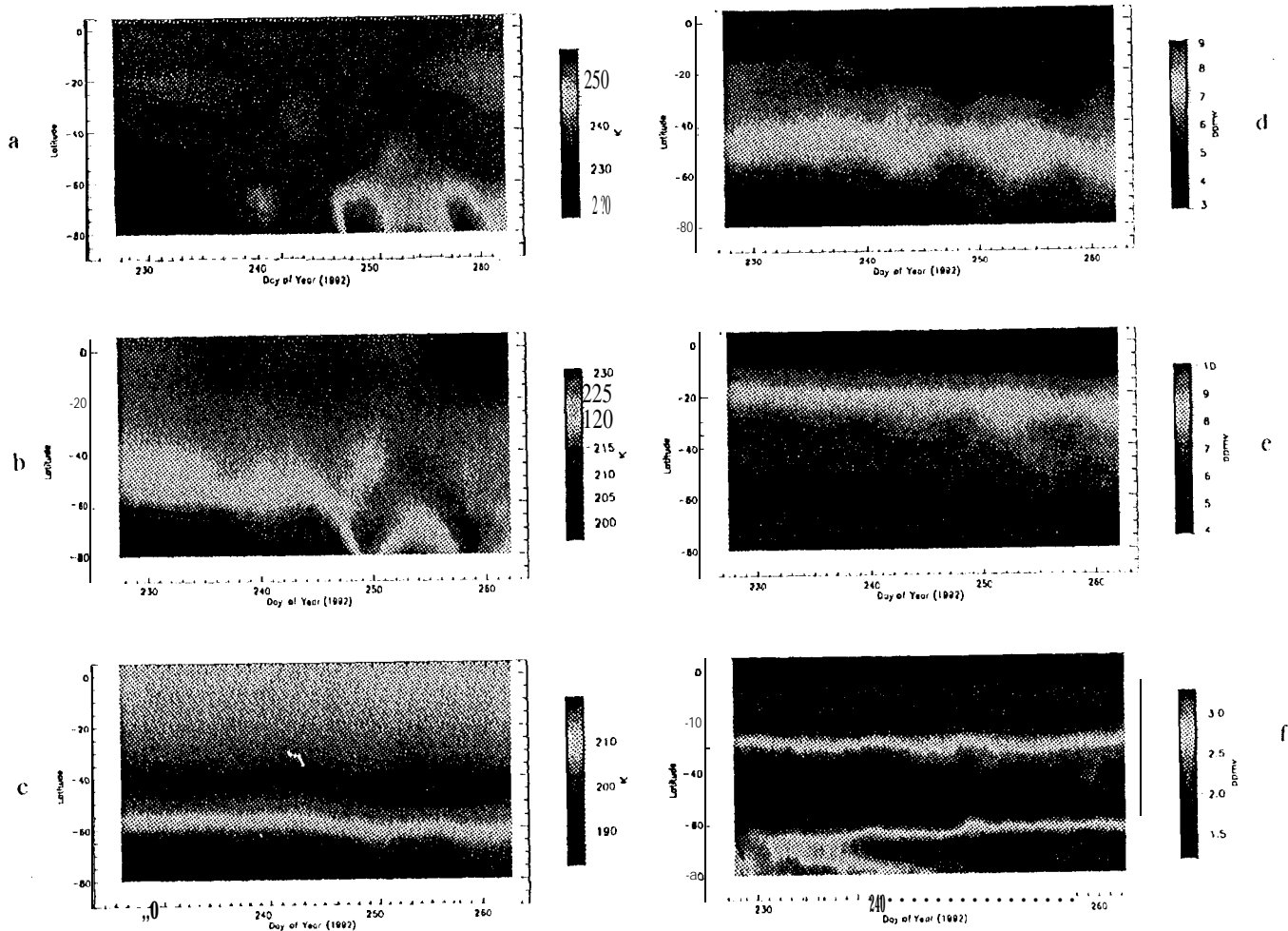


Figure 1

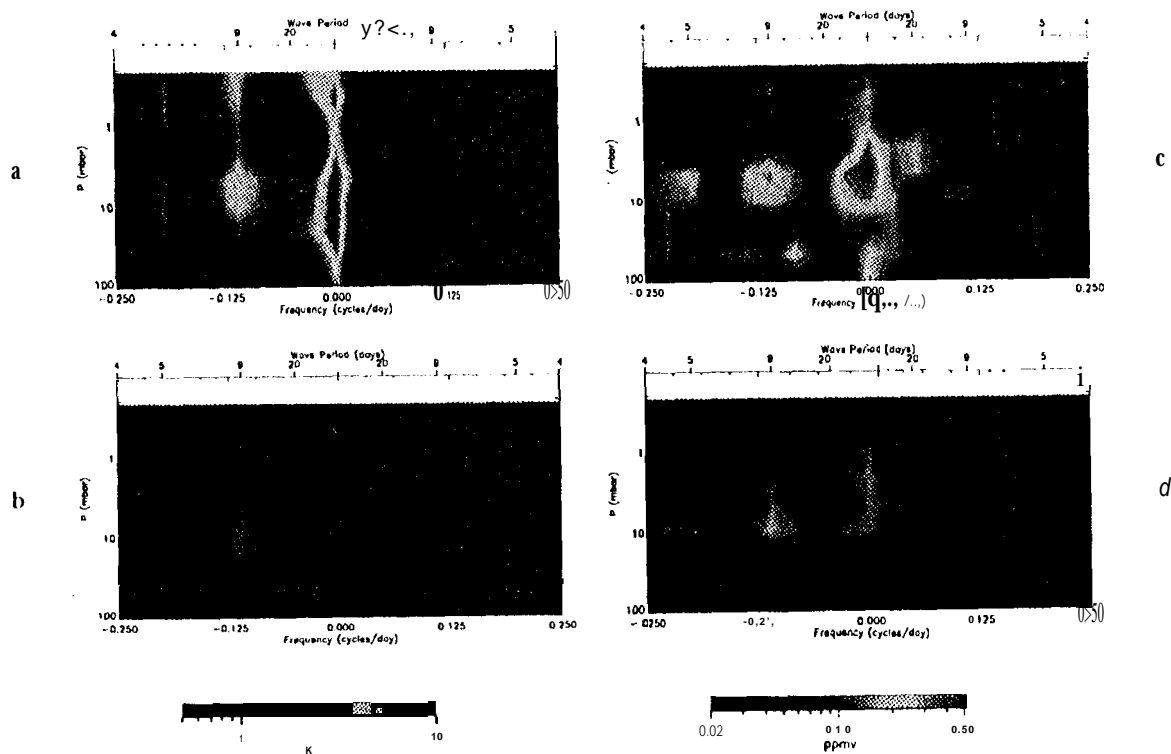


Figure 2

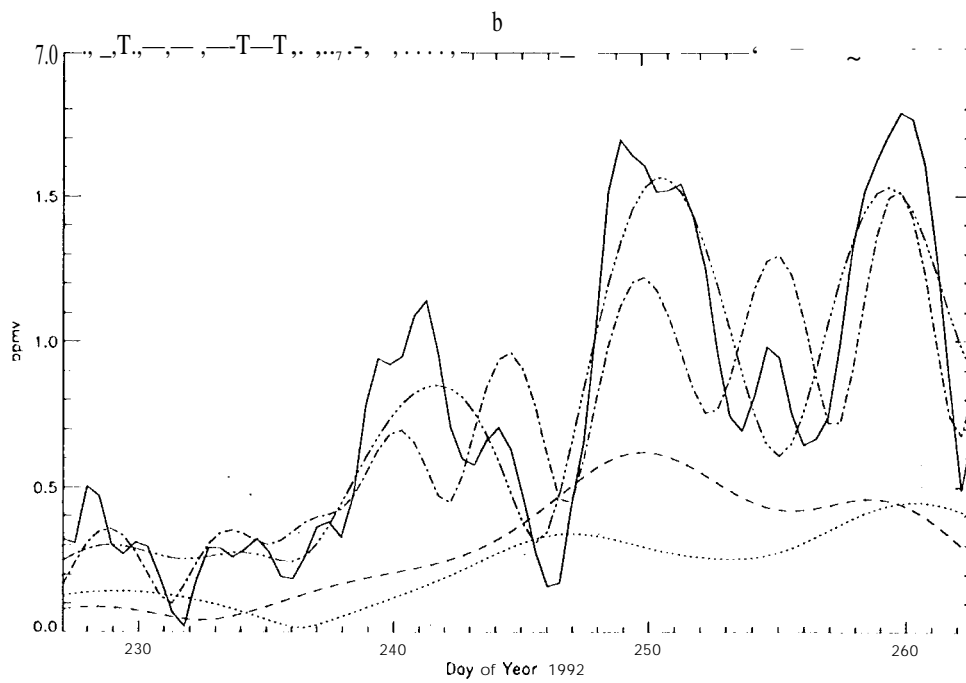
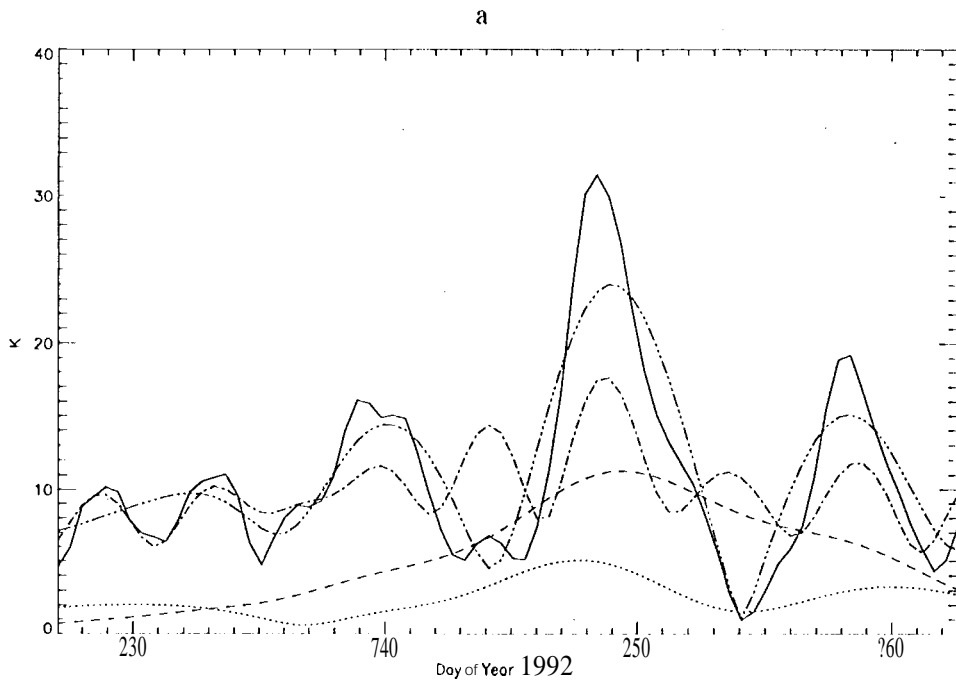


Figure 3

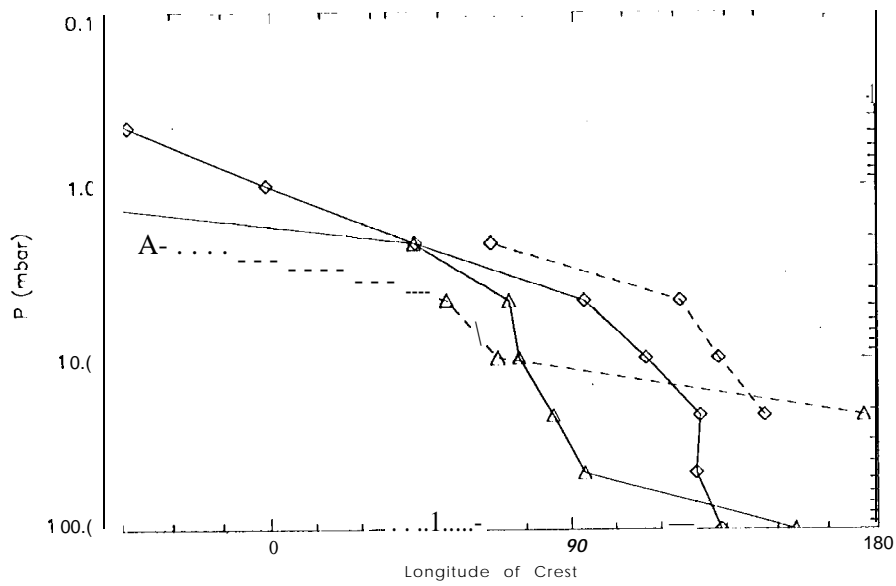


Figure 4

